Earth and Planetary Science Letters 375 (2013) 234–243

Contents lists available at ScienceDirect

Earth and Planetary Science Letters

journal homepage: www.elsevier.com/locate/epsl

Constraints on the tectonic evolution of the westernmost Mediterranean and northwestern Africa from shear wave splitting analysis

Meghan S. Miller [a,*], Amir A. Allam [a], Thorsten W. Becker [a], Jeanette F. Di Leo [b], James Wookey [b]

[a] University of Southern California, Department of Earth Sciences, 3651 Trousdale Pkwy, Los Angeles, CA 90089, USA
[b] University of Bristol, School of Earth Sciences, Wills Memorial Building, Queen's Road, Bristol BS8 1RJ, UK

ARTICLE INFO

Article history:
Received 21 March 2013
Received in revised form
17 May 2013
Accepted 21 May 2013
Editor: P. Shearer
Available online 10 July 2013

Keywords:
seismic anisotropy
subducted slab structure
mantle-flow channeling
craton–slab interaction

ABSTRACT

The westernmost Mediterranean mantle and lithosphere have evolved into their current configuration due to complex interactions between the African and Eurasian plates. To help unravel the regional tectonics, we use new broadband seismic data across the Gibraltar arc and into southern Morocco to infer azimuthal seismic anisotropy and flow patterns for the upper mantle based on shear wave splitting analysis. A deep (> 600 km) earthquake in April 2010 was recorded by the array and allowed us to compare 31 direct *S* measurements with 235 teleseismic *SK*(*K*)*S* events from 3 years of deployment. The patterns of apparent fast polarization orientations and delay times suggest three major tectonic domains when interpreted jointly with recent tomographic images of the subducted slab: (1) a subducted slab related toroidal flow domain centered upon the Alboran Sea and southern Spain, leading to complex splits, (2), a region where the west African craton deflects mantle flow in the Anti-Atlas and High Plateaux, and, (3), an intermediate domain across the central High Atlas. Across the axis of the mountain belt a coherent, regional maximum of delay times is observed for both *S* and *SKS* splitting measurements, with polarizations predominantly parallel to the strike. We interpret this as possible SW–NE channeling of mantle flow beneath the region with a thinned lithosphere and slow seismic velocities beneath the central High Atlas Mountains.

1. Introduction

The western Mediterranean and northwest Africa have a complex tectonic history that has predominantly been the result of interaction related to the European–African plate convergence during the Cenozoic (~65 Ma). The far western end of the Alpine–Himalayan orogenic belt is known as the Gibraltar arc system (Fig. 1). The region can be divided into several tectonic or orogenic domains, which can be further subdivided. The Gibraltar arc system, which includes the Rif Mountains of Morocco and the Betics in Spain, forms a tight arc around the Alboran Basin (e.g. Platt and Vissers, 1989). To the south of the Rif, the Middle Atlas and High Atlas Mountains are often grouped together. Then, farther to the south–southwest, the Anti-Atlas Mountains are the oldest mountain range in the region and extend toward the northern extent of the West African Craton (e.g. Hefferan et al., 2000). The degree to which the high topography of the entire region is the result of recent orogenesis or preservation of old structures; how mountain building has occurred, if all topography is isostatically balanced; and how deep mantle flow links to the surface deformation are all debated.

Various geological and geophysical data suggest the region has extensional features but lies within a generally compressive regime. Due to the inherent complexity of the tectonics, there have been different, and sometimes conflicting, models to explain the observations and the morphology of the tightly arcuate shaped Gibraltar arc, fast seismic velocity anomalies that extend deep into the mantle, and the presence of deep (> 600 km) focus earthquakes beneath Grenada which have occurred in 1954, 1973, 1990, 1993, and 2010 (e.g., Platt and Vissers, 1989; Blanco and Spakman, 1993; Royden, 1993; Seber et al., 1996; Lonergan and White, 1997; Comas et al., 1999; Calvert et al., 2000a; Faccenna et al., 2004; Gutscher et al., 2002; Bokelmann and Maufroy, 2007; Jolivet et al., 2009; Buforn et al., 2011; Bezada and Humphreys, 2012; Bezada et al., 2013). There is a long history of debate that includes both simple and complex models to explain the observed and inferred geodynamic features, but they can be simplified into two groups that have similar characteristics: lithospheric

* Corresponding author. Tel.: +1 213 740 6308 (office); fax: +1 213 740 0011.
E-mail address: msmiller@usc.edu (M.S. Miller).

0012-821X/$ - see front matter © 2013 Elsevier B.V. All rights reserved.
http://dx.doi.org/10.1016/j.epsl.2013.05.036

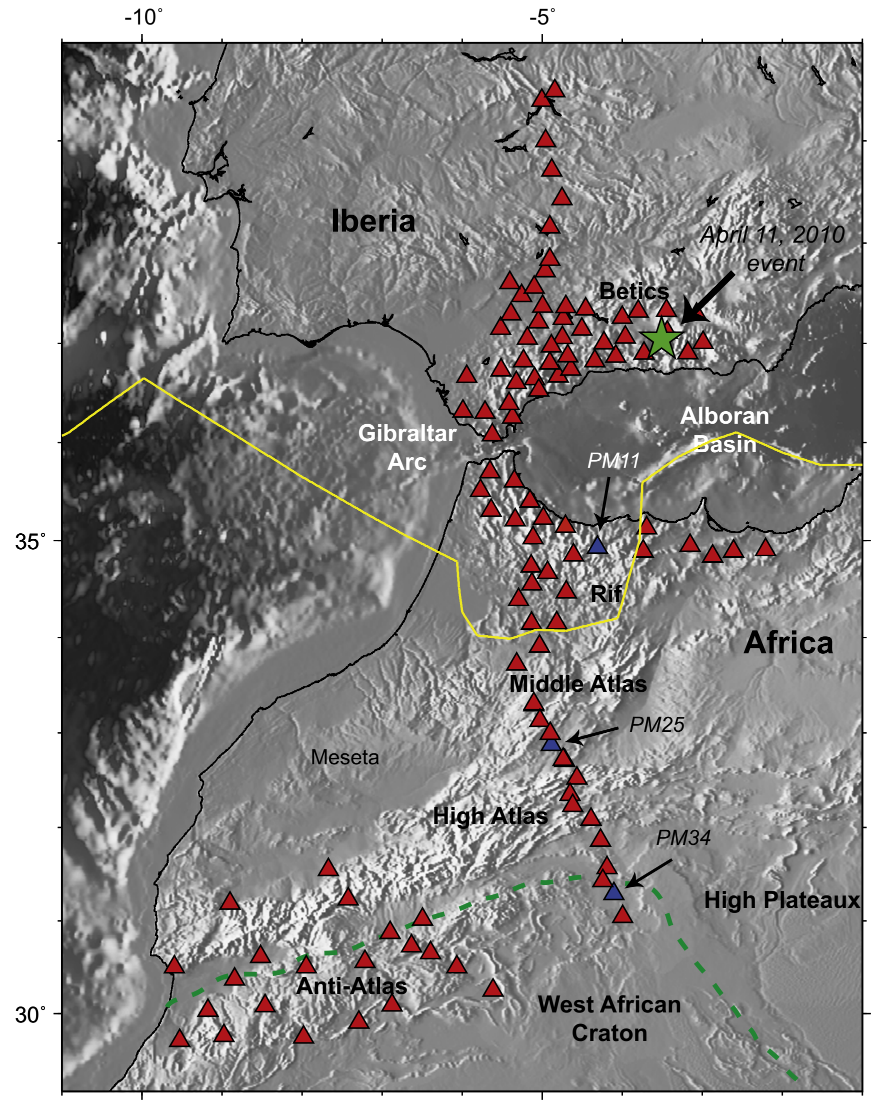

Fig. 1. Map of the western Mediterranean region with tectonic provinces, seismic station locations (triangles), major plate boundary from Bird (2003) shown as a thin yellow line, and the approximate location of the West African craton (WAC) depicted as a dashed green line. The blue triangles represent stations PM11, PM25, and PM34, for which results are shown in detail in Figs. 2 and 5. The green star is the epicenter of the deep event on April 11, 2010 used in the direct *S* analysis. (For interpretation of the references to color in this figure legend, the reader is referred to the web version of this article.)

delamination and subduction. The suggested instability mechanism leading to delamination varies, but the underlying theme of these models is basically similar, in that part of the lithosphere has been removed. The subduction models are generally based on slab rollback scenarios, where oceanic lithosphere subducts and the arc retreats. The direction of motion and dip of the slab continue to be debated, but in many of these proposed geodynamic models the slab retreats. This retreating motion then results in the crust of the overriding plate (Alboran domain) being thinned by extension.

To the south of the Betic–Rif, the Atlas Mountains are the result of reactivation of a system of failed rift basins associated with the Mesozoic opening of the central Atlantic, followed by the Cenozoic collision of Africa and Europe (e.g. Pique et al., 2002). In Morocco, the Atlas Mountains are divided into the east trending High Atlas, which reach over 4000 m, and the Middle Atlas, which reach ~3000 m and are NE trending (Fig. 1). These mountains are superimposed upon a broad topographic swell, which extends to the Meseta to the northwest and the High Plateaux to the southeast. To the southwest of the High Atlas, the older (∼600 Ma), lower topography Anti-Atlas is adjacent to northern rim of the West African Craton (WAC), which was originally part of the Pan-African orogenic belt formed as amalgamated terranes (e.g. Saquaque et al., 1989; Black et al., 1994; Hefferan et al., 2000).

Throughout the central and southern part of the study area there has been abundant alkaline to hyperalkaline magmatism during the Cenozoic, which is synchronous with plate convergence (Teixell et al., 2005; Duggen et al., 2009; and references therein). The mafic intra-continental volcanics appear to be attributed to sublithospheric melts, some of which have interacted with the overlying lithosphere, but appear to be generated at depths of 60–120 km which would normally be at depths within the continental lithosphere (Duggen et al., 2009). Geophysical observations and modeling results suggest that the lithosphere is thinned beneath the Atlas, particularly the Middle Atlas, where the lithosphere–asthenosphere boundary may be as shallow as 65 km (Seber et al., 1996; Zeyen et al., 2005; Missenard et al., 2006; Fullea et al., 2010; Anahnah et al., 2011; Jimenez-Munt et al., 2011; Miller and Butcher, 2013).

In order to understand the tectonic evolution of the western Mediterranean and northwest Africa, a large-scale network of broadband seismic stations have recently been deployed (Fig. 1) as a joint project between NSF-PICASSO, University of Münster, and Bristol University. This digital network of 105 broadband seismometers significantly extends instrumentation from Iberia and northern Morocco (Diaz et al., 2010) into southern Morocco and allows geophysical investigation of the tectonic evolution of the region.

In this study, we analyze azimuthal seismic anisotropy derived from splitting analysis of shear-waves. The origin of seismic anisotropy in the upper mantle is primarily due to lattice preferred orientation (LPO) of olivine, which may be frozen into the lithosphere or, more likely, associated with recent asthenospheric flow, which allows us to explore various tectonic models (e.g. Long and Becker, 2010; Savage, 1999; Silver, 1996). Indeed, previous studies using smaller datasets or regional subsets have used *SKS* splitting to interpret seismic anisotropy for the region (Buontempo et al., 2008; Diaz et al., 1996, 2010). A compilation of their results (Wüstefeld et al., 2009, and updates thereof) shows a dramatic rotation of the orientation of the fast polarization direction along the arc, supporting the slab rollback model rather than the lithospheric removal models for the Gibraltar arc (Diaz et al., 2010). We integrate these prior studies with our new *SKS* and direct *S* splitting results, linking mantle flow beneath and around the Alboran domain to regions farther south into Africa for the first time. The analysis of seismic anisotropy into the interior of Morocco ties together larger-scale processes driving the tectonic history of the region and inferences about the lithospheric and mantle structure of this complex region.

2. Methods

Shear waves are split into a fast and a slow pulse when propagating through azimuthally anisotropic portions of the lithosphere and upper mantle (e.g. Keith and Crampin, 1977; Bowman and Ando, 1987; Vinnik et al., 1989; Silver and Chan, 1991). The two orthogonal shear waves propagate at different velocities and are polarized into the corresponding fast (φ) and slow polarization orientations of the medium. These two waves accumulate a delay time (δt) recorded at the surface, which provides a record of the average anisotropy along the propagation path. *SKS* splitting is a particularly popular and useful observation because the *P*-to-*S* conversion at the CMB ensures the absence of source-side anisotropy, although there can be complexity in the splitting if the assumption of a single, horizontally aligned hexagonal medium is violated (e.g., Schulte-Pelkum and Blackman, 2003).

Shear wave splitting can also be observed for local events with sufficiently deep hypocenters with incidence angles less than $\sim$30–35° (Nuttli, 1961; Peacock et al., 1988; McNamara et al., 1994; Fischer and Wiens, 1996; Liu et al., 2008; Wirth and Long, 2010). However, because the propagation path of the direct *S* wave is not strictly vertical in the upper mantle, the accumulated δt and φ can reflect a different average of a potentially more complicated three-dimensional anisotropy. Additionally, the initial polarization of the direct *S* phase is unknown unless calculated from an assumed focal mechanism. Nevertheless, comparison of direct *S* and *SKS* splitting parameters can provide valuable constraints on the location of the anisotropy where the paths of the two phases coincide or where they differ slightly, for example where traveling up a slab (Fischer and Wiens, 1996), assuming that there is a single anisotropic layer with hexagonal symmetry and horizontal symmetry axis.

Splitting measurements were conducted using the MATLAB package SplitLab (Wüstefeld et al., 2008). This software simultaneously implements two different techniques for measuring the splitting parameters φ and δt in a user-selected time window: the rotation-correlation (RC) method (Bowman and Ando, 1987) and the minimum-energy method (Silver and Chan, 1991). Both techniques search for the optimum φ and δt such that horizontal particle motion for an anisotropic medium is linearized when the delayed phase has been advanced in time by δt and rotated by 90°. The two methods differ by the criterion for optimum linearization. The rotation-correlation method uses the maximum cross-correlation coefficient between all potential orthogonal horizontal components of particle motion, while the minimum-energy method searches for the lowest energy of the displacement on the corrected transverse component. In general, the observed particle motion is elliptical in the presence of anisotropy, but can be corrected by rotating the horizontal components toward the principle axis system and correcting the shift by δt, which results in backazimuth-polarized horizontal particle motion (Fig. 2a). When either a splitting or null measurement is made, it is assigned a quality of "good", "fair", or "poor", based upon signal-to-noise ratio, polarization strength of the corrected particle motion, degree of agreement between the two methods, and extent of the measurement parameter solution trade-off.

Though the assumption of an initial backazimuth polarization is valid for a spherically symmetric Earth, several factors complicate the observation of a purely backazimuth-polarized *SKS* phase: horizontal station misalignment, 3D perturbations to velocity structure, and seismic noise. Since the minimum-energy method assumes a perfectly backazimuth-oriented initial polarization, even small changes due to station misalignment or velocity structure can render the result unstable. As such, we chose the rotation-correlation as our preferred method by analyzing the waveforms, particle motion, and energy maps for both methods for all events and all stations (Fig. 2a). We note that there is generally agreement between the two methods in "good" quality measurements (Fig. S2), except those with nulls. All figures show both good and fair results from the RC method, unless noted otherwise, and the individual splitting measurements for both methods with error bounds are provided in Table S2.

3. Data and results

We apply the methodology discussed above to data from 235 global earthquakes with $M_w > 6.0$ which occurred from 2009 to 2012 at teleseismic distances between 90° and 135° from stations in Spain and Morocco. The 105 station locations are shown in Fig. 1 and are listed in Table S1. Of the initial 235 candidate teleseismic events, 123 produced data of sufficient quality to record identifiable *SKS* waves; the *SKS* waves of the remaining 112 events were either obscured by seismic noise or were not sufficiently energetic due to the source radiation pattern. To complement the *SKS* dataset we also analyzed the direct *S* wave on 32 instruments from the April 11, 2010 (617 km depth focus) earthquake that occurred beneath Grenada (e.g. Bezada and Humphreys, 2012; Buforn et al., 2011). From the 32 stations that recorded this event, 31 of the stations provided suitable data for analysis. However, following Nuttli (1961) and Fischer and Wiens (1996) we note that events with paths to the free surface should have incidence angles of 30–35° or less to avoid contamination of particle motions by converted phases and phase shifts from crustal discontinuities and the free surface. The computed incidence angles for the 26 stations with "good" results have a maximum angle of $\sim$29°, which makes these all suitable for S analysis. The locations and centroid times of the teleseismic events were based upon the global CMT catalog (Dziewonski and Woodhouse, 1983; Ekstrom et al., 2012) and theoretical arrival times for plotting and incident angle calculations were based on the 1D reference model *iasp91* (Kennett et al., 1995).

In all, 1828 *SK*(*K*)*S* (simplified as *SKS*) splits, which includes 716 null measurements, were made at 105 stations in Southern Spain

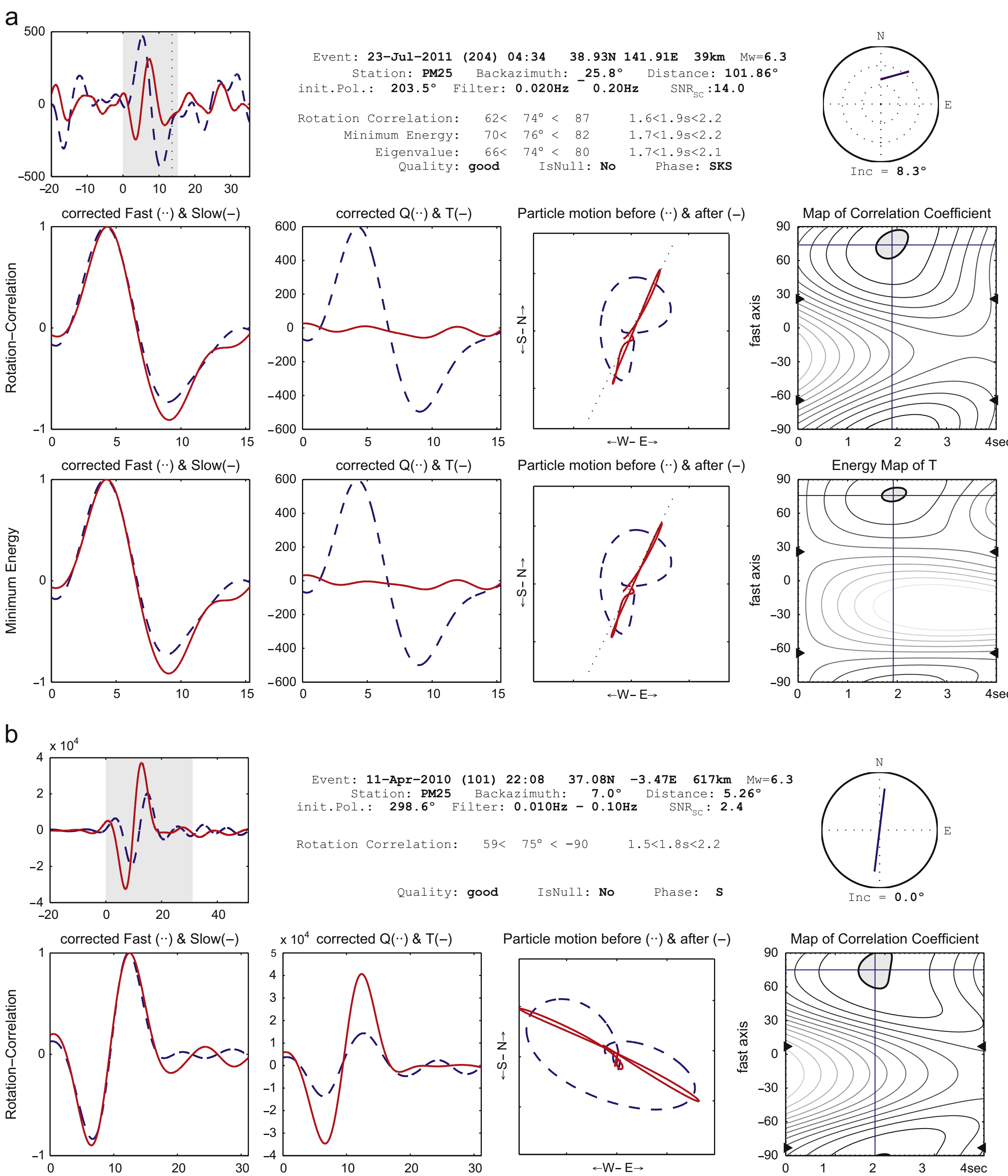

Fig. 2. Example of splitting results using SplitLab (Wüstefeld et al., 2008) for station PM25 (see Fig. 1 for location) in Morocco, (a) for *SKS* analysis and, (b) direct *S* splitting analysis. For *SKS* both rotation correlation and minimum energy computations are shown for *SKS* in (a) for completeness.

and across Morocco which were considered either “good” or “fair” (example shown in Fig. 2a). All of the measurements, including “poor” ones, are listed in Table S2 and the averages, with errors, are listed in Table S3. Of the direct *S* measurements (Table S2), eight were labeled “good”, 19 “fair”, one “poor”, and four were considered null. An example of one of these measurements is shown in Fig. 2b and others are shown in Supplementary Fig. S1.

The majority of the teleseismic events come from the NE and E (Figs. 3 and S5), but with more than 3 years of continuous data for most of the stations there is decent backazimuthal coverage. The largest delay times are at two stations in the Rif and one in the Betics (∼2.5 s), and the smallest delay times are observed at the stations that are on the West African craton (WAC) in the Anti-Atlas and south of the High Atlas (< 1 s) in the High Plateaux. The majority of the apparent fast polarization directions (FPD) from the splitting observations at the southern Moroccan stations exhibit an ENE–WSW trend that is essentially parallel to the axis of the Atlas Mountains (Figs. 3 and 4), except for those in the Rif, which have either a

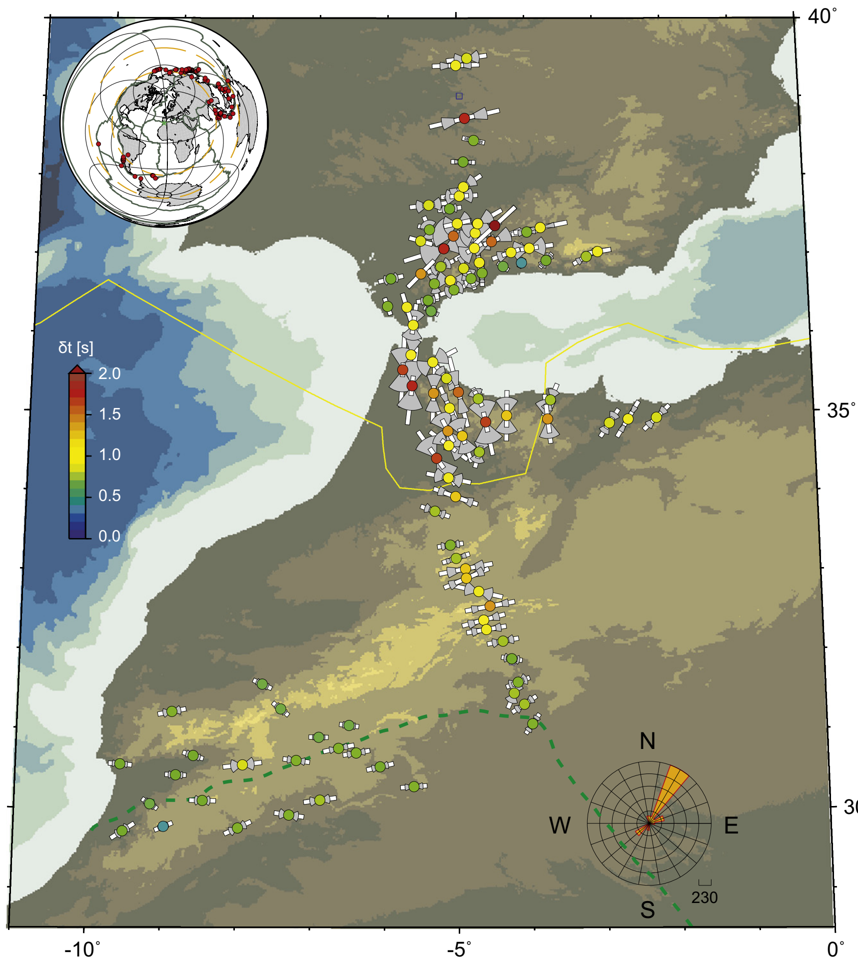

Fig. 3. Map of *SK*(*K*)*S* measurements averaged at each station. The white bars depict the magnitude of delay time and the gray wedges show the backazimuthal variations at each station. The colored dots also indicate the average delay time scaled with color. Top inset: Map of both the 123 teleseismic earthquakes (red dots) used in the analysis the location of the deep event on April 11, 2010 (green star) using in the direct *S* analysis. The orange dotted lines represent 90° and 135° from the stations and the plate boundaries are shown as dark green lines (Bird, 2003). Bottom inset: Rose diagram showing the azimuthal distribution of all the teleseismic events, with the maximum number being 230 events from the NE quadrant. (For interpretation of the references to color in this figure legend, the reader is referred to the web version of this article.)

NW–SE to N–S orientation. The direct *S* splitting results show very similar FPD orientations to the *SKS* results, except for those stations in the Rif.

4. Discussion

Most of the average *SKS* splitting results agree well with the previous *SKS* results from Diaz et al. (2010) and Buontempo et al. (2008), although there are some variations where our station spacing is denser, especially in the Rif and the Betics (Fig. 4). Further to the south, the recent deployment of stations allows for new insight into the region, which is influenced by the West African craton and the lithospheric thickness variations across the Atlas Mountains.

4.1. Rif and Betics

The new PICASSO stations are more densely spaced in the Rif and Betics (between −6°W and −4°W) than the TopoIberia stations used in Diaz et al. (2010) and the permanent stations used by Buontempo et al. (2008). Interpreting the combination of the *SKS* and direct *S* splitting observations with this array allows for a more detailed investigation of the anisotropic structure of the uppermost mantle beneath the western Mediterranean. There is a slight mismatch in the *SKS* and *S* FPD for the two stations in the Betics that recorded the deep event, but the most significant difference from previous results is the north–south oriented FPD from *SKS* splits in the Rif and internal Betics. Those are slightly different than previous results which roughly follow the Alboran Sea coastline and mountain belt topography (Fig. 4). The *SKS* splits from the Wüstefeld et al. (2009) database show a roughly symmetric horseshoe shape around the Alboran Sea (Fig. 4), but the new analysis shows a more asymmetric shape with the N-S orientations across the Rif. Our new results are a closer match to imaged *Pn* anisotropy (Calvert et al., 2000b; Diaz et al., 2013; Serrano et al., 2005), which also has a N-S orientation in the Rif, but then curves around clockwise around Gibraltar to have a E–W orientation in the Betics. However, where the *SKS* delay times are similar in both the Rif and the Betics, the *Pn* delay times are much smaller in the Rif than in the Betics.

This pattern is similar to the projection of the slab position at depth, between 250 and 500 km, as inferred from *P*-wave tomography (Bezada et al., 2013) and the circum-slab flow suggested by Diaz et al. (2010), and as explored in detailed geodynamic modeling by Alpert et al. (2013). Numerical mantle flow models that test possible density and viscosity variations in order to explore and invert for slab structures in the region suggest that there are no dense anomalies beneath the Rif at mantle depths (Alpert et al., 2013). These authors found that mantle flow models with a

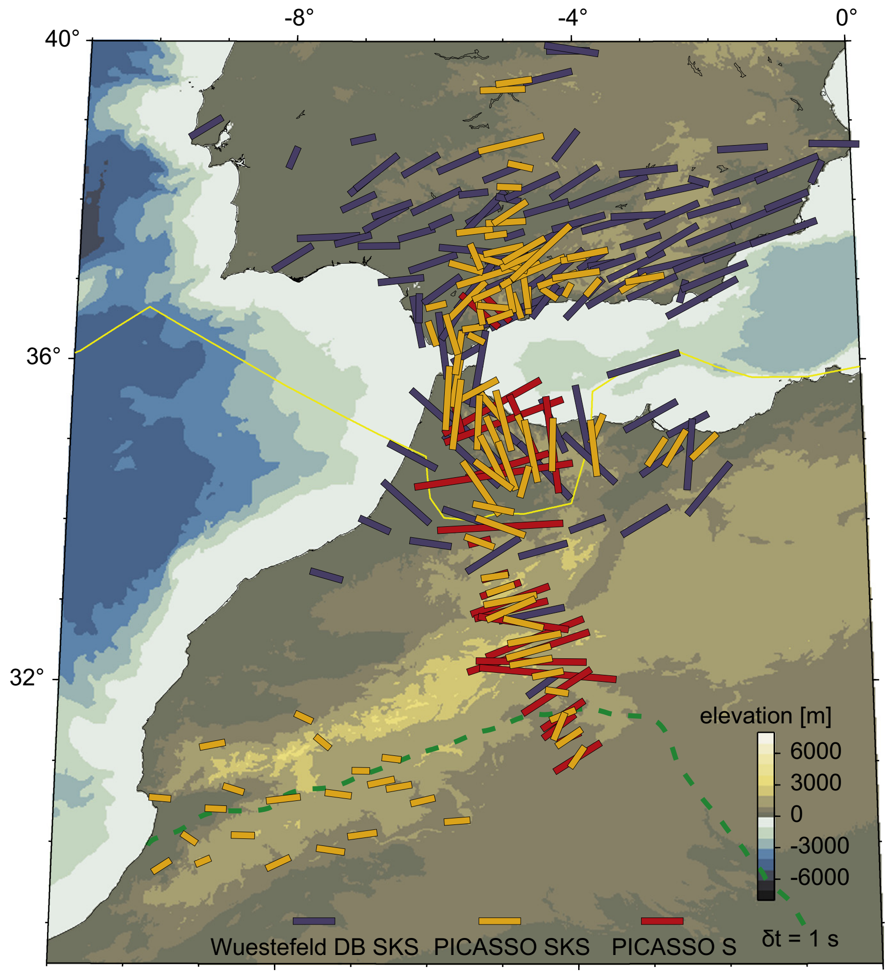

Fig. 4. Station-averaged *SK*(*K*)*S* splitting (fast polarization orientation and delay time indicated by stick azimuth and length, respectively) plotted centered at station location from the Wüstefeld et al. (2009) updated database which includes the studies of Buontempo et al. (2008) and Diaz et al. (2010) (dark blue), new *SK*(*K*)*S* (orange), and direct *S* results from the deep focus earthquake shown in Figs. 1 and 5 (red). The plate boundary is shown as thin yellow line (Bird, 2003). (For interpretation of the references to color in this figure legend, the reader is referred to the web version of this article.)

continuous slab beneath the Alboran that extended to 600 km depth – elongate along the Iberian margin between Granada to Gibraltar that is similar to the recent *P*-wave tomography images (Bezada et al., 2013) – matched a subset of the *SKS* observations from the PICASSO deployment and those previously published (Diaz et al., 2010). With the additional new seismic anisotropy measurements presented here, it is also demonstrated that the subducted slab beneath the Alboran is a primary feature that affects the mantle flow.

4.2. Subducted slab

The orientation of *SKS* and *S* inferred fast-polarization directions (FPD) are mostly similar across the region, except for the stations in the Rif Mountains (Fig. 4). We suggest that this inconsistency is due to the interaction of the direct *S* wave traveling up the slab from its origin at >600 km depth for the Rif stations. As shown in Figs. 5, S1 and S4, the *S* and *SKS* raypaths to Rif and Atlas stations are significantly different and traverse different amounts or portions of the fast velocity material as imaged in the *P*-wave tomography (Bezada et al., 2013).

Fig. 5 shows examples of measurements, ray paths, and cross sections through the tomographic model for stations PM11 in the Rif, PM25 in the Middle Atlas, and PM34 on the High Plateaux. The ray paths to the stations outside of the Rif and Betics are inferred to sample more of the “normal” mantle, which is similar to the paths that the teleseismic *SKS* waves take to these stations. The paths to the Rif stations are likely to cross a much more complex and heterogeneous upper mantle structure, which is dominated by the fast velocities associated with the slab beneath the Alboran. This suggests that the cause of the discrepancy between the Betics, Rif and Atlas stations for the direct *S* splitting versus *SKS* splitting results is the position and continuous nature of the fast velocity material beneath the Alboran and northernmost Morocco (Supplementary Fig. 2).

Fig. 5a shows that the raypaths for both the direct *S* and the teleseismic *SKS* phases from the NE quadrant (shown in yellow) travel entirely through the fast velocity material of the subducted slab to PM11. The *SKS* raypaths for events from the SW (shown in orange) do not pass through the fast velocity material and therefore have a very different apparent fast polarization orientation and smaller delay time. In contrast, all the events recorded at PM25 in the Middle Atlas, both direct *S* and *SKS*, have ray paths that miss the fast material for much of the upper mantle, but all cross through very slow velocity uppermost mantle. This results in very similar orientation and delay time of the splitting measurements. However, the ray paths for both the *SKS* and deep focus *S* events recorded at PM34, at the edge of the West African Craton (WAC) and on the High Plateaux, do not travel through a significant amount (or any) of the fast velocity material in the

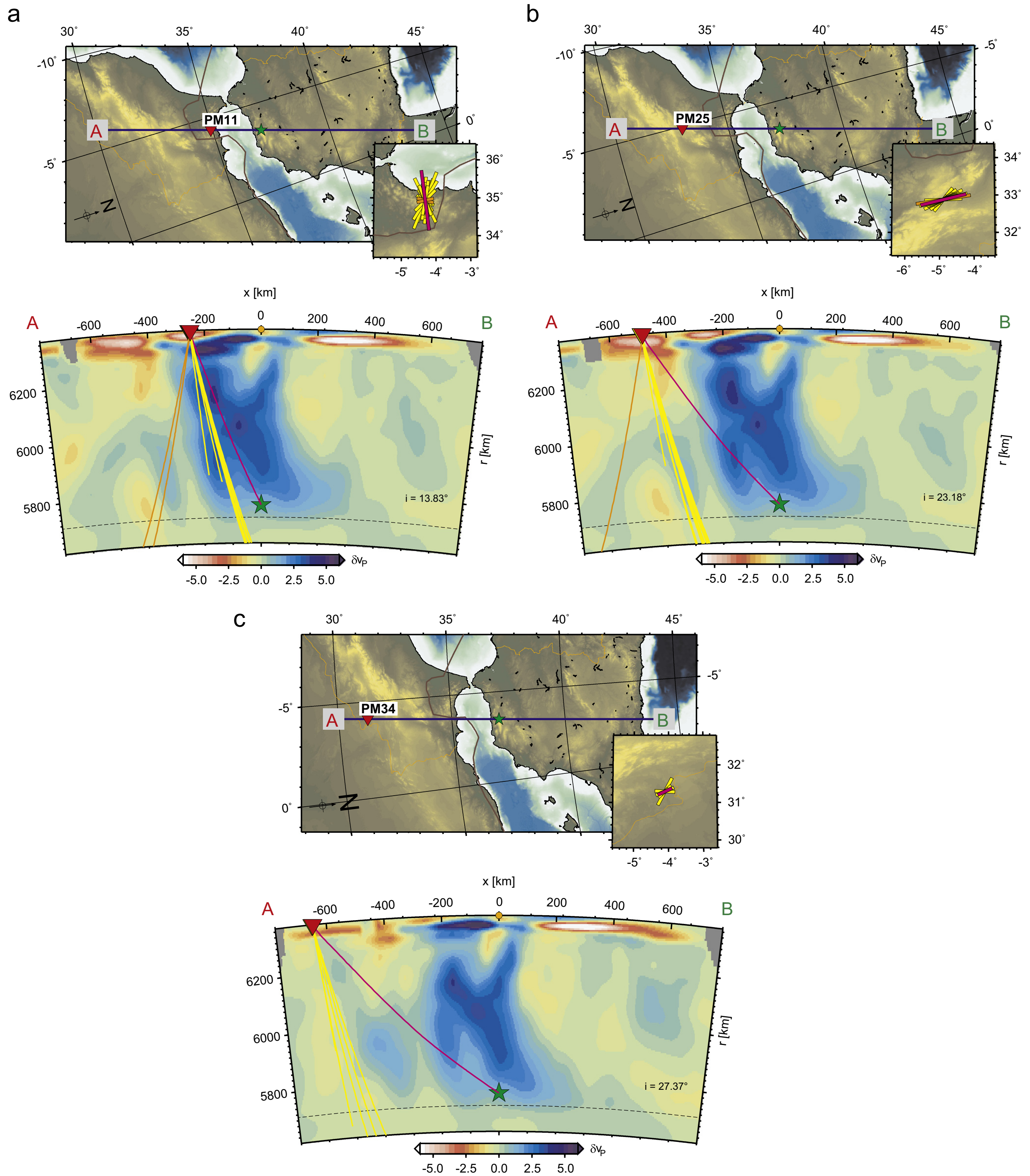

Fig. 5. Map and cross sections along profile A–B through the *P*-wave tomography model of Bezada et al. (2013) with the location of the deep focus event (green star) and raypath (magneta line) that occurred on April 11, 2010 recorded at: (a) station PM11 in the Rif mountains and, (b) station PM25 in the Middle Atlas and (c) PM34 in the Sahara as indicated by the red inverted triangles. The raypaths for the events that travel within 1° of the profile are plotted with the tomography and are colored by backazimuth (arrival from south and northern hemisphere shown yellow and orange, respectively). The corresponding splitting measurements are shown as an inset within each of the figures and are also colored by azimuth and local event (magneta). The incidence angle for the deep focus event is shown indicated as "i" in the lower right corner. (For interpretation of the references to color in this figure legend, the reader is referred to the web version of this article.)

mantle associated with the subducted slab, but have similar delay times and orientation. This results again in very similar orientations and delay time measurements.

To the south of the Rif and north of the Middle Atlas, both the *SKS* and direct *S* results show an interesting change in orientation south of ~34°N (Figs. 3 and 4), which is located near the inferred plate boundary of Bird (2003). It is also the inferred boundary between the Rif and the rest of Morocco from analysis of geodetic data (Koulali et al., 2011), as the Rif "block" appears to be moving separately from the rest of North Africa. Recent *P*-wave tomography images show that the fast velocity perturbations associated with the attached subducted slab extend almost as far south as the inferred plate boundary, but have complex heterogeneities at depth (Figs. 5 and S4). This suggests that the splitting measurements change across 34°N due to the change in flow patterns at the edge of the slab in Northern Morocco.

As previously mentioned, the position and presence of a subducted slab beneath the Alboran Sea has been debated (Blanco and Spakman, 1993; Bokelmann and Maufroy, 2007; Calvert et al., 2000a; Gutscher et al., 2002). This change in orientation in the direct *S* splitting observations can be used as another piece of evidence for the slab position and morphology at depth. Further evidence lies in the multipathing effects of the *S* waves traveling up the slab versus those that traverse the edge of the slab (Sun and Miller, 2013).

4.3. Central High Atlas Mountains

The splitting results for both *S* and *SKS* across the High Atlas show a change in delay time from north to south (Figs. 3 and 4). Most interestingly, the peak ($\sim$3 s average for *S* and $\sim$1.5 s for *SKS*) in magnitude occurs along the axis of the High Atlas, where the elevation is highest. On the flanks of each side of the mountain range, the Middle Atlas to the north and the High Plateaux to the south, the magnitudes of the delay time decrease (0.5–1.0 s). Fig. S5 shows the individual splitting results plotted at 200 km depth along each event's raypath for the *SKS* results and at the station location for the direct *S* results. Although the majority of the events come from the NE (Figs. 3 and S5), both the delay time (δt) and orientation (φ) are similar between *S* and *SKS* for all the events analyzed in the central Atlas.

We speculate that this may be related to the variation in thickness of the lithosphere, which has been suggested to be shallow ($\sim$65 km) beneath the Atlas and thickest ($\sim$120 km) beneath the Rif (Anahnah et al., 2011; Fullea et al., 2010; Jimenez-Munt et al., 2011; Miller and Butcher, 2013; Missenard et al., 2006; Zeyen et al., 2005). Previous authors have proposed that a mantle plume might interact with a thinned lithosphere, interplate volcanism, and seismicity (Missenard et al., 2006; Teixell et al., 2005). This plume material could be from the Canary Islands and been channeled in a sub-lithospheric corridor where the volcanics indicate a geochemical mixing trend with Canary Island volcanics an end-member (Duggen et al., 2009). Fig. 5b also illustrates the significant amount of slow velocity material beneath the Middle and Central Atlas as inferred from *P*-wave tomography. At stations above this region (PM25–29 for example) we have the largest magnitude splitting measurement (Figs. 3, 4, S3, and S5). This suggests that there may be melt and/or a thick region of flowing asthenosphere where the majority of the seismic anisotropy signal originates. However, the splitting delay times are much smaller for the western High Atlas, ($<\sim$1 s) which makes it more challenging to infer a continuous channel from the Canary Islands, as suggested by Duggen et al. (2009). This might indicate a discontinuous channel, or contamination of the asthenospheric seismic anisotropy signal by frozen-in anisotropy in the lithosphere. A connection between the Canary plume, lithospheric thinning and subduction dynamics is therefore not straight forward nor universally accepted, but, to us, a plausible overall explanation for a range of observations.

4.4. Anti-Atlas Mountains

Similar to the southernmost splitting results for stations in the High Plateaux on the edge of the craton (PM32 through PM35), the Anti-Atlas stations have an average splitting magnitude of less than 1 s and apparent fast polarization orientations that are approximately parallel to the axis of the mountain range (Figs. 3 and 4). The observed, relatively small amplitude splitting results could be due to fossil anisotropy in the lithosphere (e.g. Fouch and Rondenay, 2006; Bastow et al., 2007), rather than present-day mantle flow, which dominates the signal in the other northern portions of the study area. As the orientations of the splitting results in the Anti-Atlas and Atlas mirror the trend of the surface geology, which primarily consist of exposed Pan-African, Paleozoic fold belts (i.e. Hefferan et al., 2000), it is plausible that the anisotropy inferred is from the remnant strain in the continental interior (craton) from the last deformational event (Silver and Chan, 1991; Bastow et al., 2007). However, when compared to the modeling results of Alpert et al. (2013), we favor the interpretation that these signals are likely to be due to the effect of the West African craton and the subducted–slab beneath the Alboran deflecting the mantle flow to the north-northeast beneath the region of thin lithosphere. Alpert et al. (2013) used global mantle flow calculations to predict the resulting LPO anisotropy (cf. Becker et al., 2006; Miller and Becker, 2012) and compared their models with a subset of the average *SKS* splitting observations for the region. Their best-fit model is able to match the large magnitude splitting for the Atlas and change to smaller delay times in the High Plateaux if an arcuate slab comparable to the tomographically imaged structure (Bezada et al., 2013) is included as a sinker, as well as a stiff continental keel in southwestern Morocco. The superposition of large-scale plate motion associated shear, flow induced by the dense slab and the stiff continental keel lead to flow that parallels the Atlas Mountains. However, the lithosphere in these models is assumed to be homogeneously 100 km thick, which may be too simplified given prior suggestions and our detailed analysis of the new splitting results, which include the direct *S* observations. The further exploration of an optimized geodynamic model for the Atlas–craton interactions within the context of dynamic support of the Atlas appears a useful future line of inquiry.

5. Conclusions

Analysis of *SKS* and direct *S* waves at 105 densely spaced broadband seismic stations from Iberia to southern Morocco provide an improved understanding of the seismic anisotropy, mantle flow, and tectonic history of the western Mediterranean. We confirm the overall arcuate splitting pattern across Gibraltar and the Alboran Sea, presumably related to toroidal flow around a subducted slab as inferred by fast velocity perturbations in tomographic images and geodynamic models. However, our new results reveal more detail and complexity in the Rif and Betics than had previously been suggested. In particular, the local *S* arrivals (which sample the inferred slab in the upper mantle into the transition zone) indicate complex anisotropy at depth. Seismic data recorded at new stations in the Atlas and Anti-Atlas Mountains in Morocco show that fast polarization directions are parallel to the axes of the highest topography across the central High Atlas, and there are significant and consistent variations in delay time patterns both in direct *S* and teleseismic *SKS* phases. The region of largest inferred anisotropy coincides with domains where thinned lithosphere has been suggested, indicating possible channelized flow along the orogen, or at least the region that has very slow *P*-wave velocities. Further south, delay times decrease toward Algeria in the High Plateaux, and show some complexity in small magnitude splitting observations in the Anti-Atlas which may be related to frozen-in anisotropy close to the northern margin of West African craton. Our analysis indicates that lithospheric deformation and mantle flow are influenced by the presence of a subducted slab beneath the Alboran, the variation in lithospheric thickness across Morocco, and the presence of the old, stable, continental craton of northwestern Africa.

Acknowledgments

This study was supported by the National Science Foundation, Continental Dynamics Program, under EAR-0809023, and by the European Research Council, under grant agreement 240473 "CoMITAC". We thank C. Thomas for sharing her seismic data from the Anti-Atlas, and a special thanks to IRIS PASSCAL, C.P. Ryan, M. Harnafi, D. Elouai, and all the people at L'Institut Scientifique at Mohammad V University in Rabat who made the experiment possible. We thank J. Diaz for initial discussions about the results, and thank J. Platt, C. Faccenna and L. Moresi for their input on discussions about early versions of the manuscript. We also thank the two anonymous reviewers who provided excellent, detailed suggestions and comments, which greatly improved and strengthened the manuscript.

Appendix A. Supplementary materials

Supplementary data associated with this article can be found in the online version at http://dx.doi.org/10.1016/j.epsl.2013.05.036.

References

Alpert, L.A., Miller, M.S., Becker, T.W., A.A., 2013., Structure beneath the Alboran from geodynamic flow models and seismic anisotropy, *J. Geophys. Res*, in review.
Anahnah, F., Galindo-Zaldivar, J., Chalouan, A., Pedrera, P., Ruano, J., Pous, J., Heise, W., Ruiz-Constan, A., Benmakhlouf, M., López-Garrido, A.C., Ahmamou, M.F., Sanz de Galdeano, C., Arzate, J., Ibarra, P., González-Castillo, L., Bouregba, N., Corbo, F., Asensio, E., 2011. Deep resistivity cross section of the intraplate Atlas Mountains (NW Africa): new evidence of anomalous mantle and related Quaternary volcanism. Tectonics 30 (TC5014), http://dx.doi.org/10.1029/2010TC002859.
Bastow, I.D., Owens, T.J., Helffrich, G., Knapp, J.H., 2007. Spatial and temporal constraints on sources of seismic anisotropy: evidence from the Scottish highlands. Geophys. Res. Lett. 34, L05305 10.1029/2006GL028911.
Becker, T.W., Schulte-Pelkum, V., Blackman, D.K., Kellogg, J.B., O'Connell, R.J., 2006. Mantle flow under the western United States from shear wave splitting. Earth Planet. Sci. Lett. 247, 235–251.
Bezada, M.J., Humphreys, E.D., 2012. Contrasting rupture processes during the April 11, 2010 deep-focus earthquake beneath Granada, Spain. Earth Planet. Sci. Lett. 353, 38–46.
Bezada, M.J., Humphreys, E.D., Toomey, D.R., Harnafi, M., Dávila, J.M., Gallart. J., J., 2013. Evidence for slab rollback in the westernmost Mediterranean from improved upper mantle imaging. Earth Planet. Sci. Lett. 368, 51–60, http://dx.doi.org/10.1016/j.epsl.2013.02.024.
Bird, P., 2003. An updated digital model of plate boundaries. Geochem. Geophys. Geosyst. 4, 1027, http://dx.doi.org/10.1029/2001GC000252.
Black, R., Latouche, L., Liegeois, J.P., Caby, R., Bertrand, J.M., 1994. Pan-African displaced terranes in the Tuareg shield (central Sahara). Geology 22, 641–644.
Blanco, M., Spakman, W., 1993. The P-wave velocity structure of the mantle below the Iberian Peninsula: evidence for subducted lithosphere below southern Spain. Tectonophysics 221, 13–34.
Bokelmann, G., Maufroy, E., 2007. Mantle structure under Gibraltar constrained by dispersion of body waves. Geophys. Res. Lett. 34 (L22305), http://dx.doi.org/10.1029/2007GL030964.
Bowman, J.R., Ando, M., 1987. Shear-wave splitting in the upper-mantle wedge above the Tonga subduction zone. Geophys. J. R. Astron. Soc. 88, 25–41.
Buforn, E., Pro, C., Cescam, S., Udias, A., del Fresno, C., 2011. The 2010 Granada, Spain, deep earthquake. Bull. Seismol. Soc. Am. 101, 2418–2430.
Buontempo, L., Bokelmann, G.H.R., Barruol, G., Morales, J., 2008. Seismic anisotropy beneath southern Iberia from SKS splitting. Earth Planet. Sci. Lett. 273, 237–250.
Calvert, A., Sandvol, E., Seber, D., Barazangi, M., 2000a. Geodynamic evolution of the lithosphere and upper mantle beneath the Alboran region of the western Mediterranean: constraints from travel time tomography. J. Geophys. Res. 105, 10871–10898.
Calvert, A., Sandvol, E., Seber, D., Barazangi, M., Vidal, F., Alguacil, G., Jabour, N., 2000b. Propagation of regional seismic phases (Lg and Sn) and Pn velocity structure along the Africa–Iberia plate boundary zone: tectonic implications. Geophys. J. Int. 142, 384–408.
Comas, M.C., Platt, J.P., Soto, I., Watts, A.B., 1999. The origin and tectonic history of the Alboran basin: insights from leg 161 results. In: Proceedings of the Ocean Drilling Program, Scientific Results, vol. 161, pp. 555–579.
Diaz, J., Hirn, A., Gallart, J., Abalos, B., 1996. Upper-mantle anisotropy in SW Iberia from long-range seismic profiles and teleseismic shear-wave data. Phys. Earth Planet. Inter. 95, 153–166.
Diaz, J., Gallart, J., Villaseñor, A., Mancilla, F., Pazos, A., Córdoba, D., Pulgar, J.A., Ibarra, P., Harnafi, M., 2010. Mantle dynamics beneath the Gibraltar Arc (western Mediterranean) from shear-wave splitting measurements on a dense seismic array. Geophys. Res. Lett. 37 , (L18304), http://dx.doi.org/10.1029/2010GL044201.
Diaz, J., Gil, A., Gallart, J., 2013. Uppermost mantle seismic velocity and anisotropy in the Euro-Mediterranean region from Pn and Sn tomography. Geophys. J. Int. 192, 310–325.
Duggen, S., Hoernle, K.A., Hauff, F., Klügl, A., Bouabdellah, M., Thirlwall, M., 2009. Flow of Canary mantle plume material through a subcontinental lithospheric corridor beneath Africa to the Mediterranean. Geology 37 (3), 283–286.
Dziewonski, A.M., Woodhouse, J.H., 1983. An experiment in systematic study of global seismicity: centroid-moment tensor solutions for 201 moderate and large earthquakes of 1981. J. Geophys. Res. 88, 3247–3271.
Ekstrom, G., Nettles, M., Dziewonski, A.M., 2012. The global CMT project 2004–2012: centroid-moment tensors for 13,017 earthquakes. Phys. Earth Planet. Inter. 200–201, 1–9.
Faccenna, C., Piromallo, C., Crespo-Blanc, A., Jolivet, L., Rossetti, F., 2004. Lateral slab deformation and the origin of the western Mediterranean arcs. Tectonics 23 , (TC1012), http://dx.doi.org/10.1029/2002TC001488.
Fischer, K.M., Wiens, D.A., 1996. The depth distribution of mantle anisotropy beneath the Tonga subduction zone. Earth Planet. Sci. Lett. 142, 253–260.
Fouch, M.J., Rondenay, S., 2006. Seismic anisotropy beneath stable continetal interiors. Phys. Earth Planet. Lett. 158, 292–320.
Fullea, J., Fernandez, M., Afonso, J.C., Verges, J., Zeyen, H., 2010. The structure and evolution of the lithosphere–asthenosphere boundary beneath the Atlantic–Mediterranean Transition Region. Lithos 120 (1–2), 74–95.
Gutscher, M.-A., Malod, J., Rehault, J.-P., Contrucci, I., Klingelhoefer, K., Mendes-Victor, L., Spakman, W., 2002. Evidence for active subduction beneath Gibraltar. Geology 30 (12), 1071–1074.
Hefferan, K.P., Admou, H., Karson, J.A., Saquaque, A., 2000. Anti-Atlas (Morocco) role in Neoproterozoic Western Gondwana reconstruction. Precambrian Res. 103, 89–96.
Jimenez-Munt, I., Fernandez, M., Verges, J., Garcia-Castellanos, D., Fullea, J., Perez-Gussinye, M., Afonso, J.C., 2011. Decoupled crust–mantle accommodation of Africa–Eurasia convergence in the NW Moroccan margin. J. Geophys. Res. 116 , (B08403), http://dx.doi.org/10.1029/2010JB008105.
Jolivet, L., Faccenna, C., Piromallo, C., 2009. From mantle to crust: stretching the Mediterranean. Earth Planet. Sci. Lett. 285 (1–2), 198–209.
Kennett, B.L.N., Engdahl, E.R., Buland, R., 1995. Constraints on seismic velocities in the Earth from travel times. Geophys. J. Int. 122, 108–124.
Keith, C.M., Crampin, S., 1977. Seismic body waves in anisotropic media: synthetic seismograms. Geophys. J. R. Astron. Soc. 49, 225–243.
Koulali, A., Ouazar, D., Tahayt, A., King, D.W., Vernant, P., Reilinger, R., McClusky, S., Mourabit, T., Davila, J.M., Amraoui, N., 2011. New GPS constraints on active deformation along the Africa–Iberia plate boundary. Earth Planet. Sci. Lett. 308 (1–2), 211–217.
Liu, K.H., Gao, S.S., Gao, Y., Wu, J., 2008. Shear wave splitting and mantle flow associated with the deflected Pacific slab beneath northeast Asia. J. Geophys. Res. 113 , (B01305), http://dx.doi.org/10.1029/2007JB005178.
Lonergan, L., White, N., 1997. Origin of the Betic-Rif mountain belt. Tectonics 16, 504–522.
Long, M.D., Becker, T.W., 2010. Mantle dynamics and seismic anisotropy. Earth Planet. Sci. Lett. 297, 341–354.
McNamara, D.E., Owens, T.J., Silver, P.G., Wu, F.T., 1994. Shear wave anisotropy beneath the Tibetan Plateau. J. Geophys. Res. 99, 13,655–613,665.
Miller, M.S., Becker, T.W., 2012. Mantle flow deflected by interactions between subducted slabs and cratonic keels. Nat. Geosci. 10, 726–730.
Miller, M.S., Butcher, A., 2013. Investigating and Imaging the Lithospheric Structure of the Westernmost Mediterranean Using S Receiver Functions, EGU General Assembly 2013, Vienna.
Missenard, Y., Zeyen, H., Frizon de Lamotte, D., Leturmy, P., Petit, C., Sebrier, M., Saddiqi, O., 2006. Crustal versus asthenospheric origin of relief of the Atlas Mountains of Morocco. J. Geophys. Res. 111, (B03401), http://dx.doi.org/10.1029/2005JB003708.
Nuttli, O., 1961. The effect of the Earth's surface on the S wave particle motion. Bulletin of the Seismological Society of America 51, 237–246.
Peacock, S.M., Crampin, S., Booth, D.C., Fletcher, R.C., 1988. Shear wave splitting in the Anza seismic gap, southern California: temporal variations as possible precursors. J. Geophys. Res. 93 (B4), 3339–3356.
Pique, A., Tricart, P., Guiraud, R., Laville, E., Bouaziz, S., Amrhar, M., Ait Ouali, R., 2002. The Mesozoic–Cenozoic Atlas belt (North Africa): an overview. Geodinamica Acta 15 (3), 185–208.
Platt, J.P., Vissers, R.L.M., 1989. Extensional collapse of thickened continental lithosphere: a working hypothesis for the Alboran sea and Gibraltar arc. Geology 17, 540–543.
Royden, L.H., 1993. The tectonic expression of slab pull at continental convergent boundaries. Tectonics 12, 303–325.

Saquaque, A., Admou, H., Karson, J.A., Hefferan, K., Reu-ber, I., 1989. Precambrian accretionary tectonics in the Bou Azzer–El Graara region, Anti-Atlas Morocco. Geology 17, 1107–1110.
Savage, M.K., 1999. Seismic anisotropy and mantle deformation: what have we learned from shear wave splitting? Rev. Geophys. 37, 65–106.
Schulte-Pelkum, V., Blackman, D.K., 2003. A synthesis of seismic P and S anisotropy. Geophys. J. Int. 154, 166–178.
Seber, D., Barazangi, M., Ibenbrahim, A., Demnati, A., 1996. Geophysical evidence for lithospheric delamination beneath the Alboran Sea and Rif–Betic mountains. Nature 379, 785–790.
Serrano, I., Hearn, T.M., Morales, J., Torcal, F., 2005. Seismic anisotropy and velocity structure beneath the southern half of the Iberian Peninsula. Phys. Earth Planet. Inter. 150, 317–330.
Silver, P.G., Chan, W.W., 1991. Shear wave splitting and subcontinental mantle deformation. J. Geophys. Res. 96 (B10), 16429–16454.
Silver, P.G., 1996. Seismic anisotropy beneath the continents: probing the depths of geology. Annu. Rev. Earth Planet. Sci. 24, 385–432.
Sun, D., Miller, M.S., 2013. Study of the western edge of the African Large Low Shear Velocity Province. Geochem. Geophys. Geosyst., 14, http://dx.doi.org/10.1002/ggge.20185.
Teixell, A., Ayarza, P., Zeyen, H., Fernandez, M., Arboleya, M.-L., 2005. Effects of mantle upwelling in a compressional setting: the Atlas Mountains of Morocco. Terra Nova 17, 456–461.
Vinnik, L.P., Farra, V., Romanowicz, B., 1989. Azimuthal anisotropy in the Earth from observations of SKS at Geoscope and NARS broadband stations. Bull. Seismol. Soc. Am. 79, 1542–1558.
Wirth, E., Long, M.D., 2010. Frequency-dependent shear wave splitting beneath the Japan and Izu-Bonin subduction zones. Phys. Earth Planet. Inter. 181 (3), 141–154.
Wüstefeld, A., Bokelmann, G., Zaroli, C., Barruol, G., 2008. SplitLab: a shear-wave splitting environment in Matlab. Comput. Geosci. 34, 518–528.
Wüstefeld, A., Bokelmann, G.H.R., Barruol, G., Montagner, J.P., 2009. Identifying global seismic anisotropy patterns by correlating shear-wave splitting and surface-wave data. Phys. Earth Planet. Inter. 176, 198–212.
Zeyen, H., Ayarza, P., Fernandez, M., Rimi, A., 2005. Lithospheric structure under the western African–European plate boundary: a transect across the Atlas Mountains and the Gulf of Cadiz. Tectonics 24, (TC2001), http://dx.doi.org/10.1029/2004TC001639.